

boundary surface. The instability is accompanied by a negative voltage spike and is preceded by helical magnetic perturbations, as observed also in other experiments. The instability itself is an expansion of the plasma minor radius which is symmetric in minor azimuth; the expansion velocity is slow compared to the ion sound speed, and it begins at or inside the  $q = 1$  surface. It is unlikely that the disruption depends on the plasma-wall interaction.

\*Work supported in part by the U. S. Atomic Energy Commission under Contract No. AT(04-3)-167, Project Agreement No. 38, and in part by Electric Power Research Institute-Edison Electric Institute Agreement No. RP-115.

†On leave from the Institute of Plasma Physics, Nagoya University, Nagoya, Japan.

<sup>1</sup>T. Ohkawa, M. Yoshikawa, R. E. Kribel, A. A. Schupp, and T. H. Jensen, *Phys. Rev. Lett.* **24**, 95 (1970).

<sup>2</sup>D. M. Meade *et al.*, in Proceedings of the Fifth International Conference on Plasma Physics and Controlled Nuclear Fusion Research, Tokyo, Japan, 1974 (International Atomic Energy Agency, Vienna, Austria, to be published), Paper No. A15-4.

<sup>3</sup>G. V. Sheffield, Princeton University Plasma Physics Laboratory Report No. MATT-999, 1973 (unpublished).

<sup>4</sup>V. D. Shafranov, *Zh. Tekh. Fiz.* **43**, 225 (1971) [*Sov. Phys. Tech. Phys.* **18**, 151 (1973)].

<sup>5</sup>J. C. Hosea, F. C. Jobes, R. L. Hickok, and A. N. Dellis, *Phys. Rev. Lett.* **30**, 839 (1973).

<sup>6</sup>Robert A. Jacobson, Princeton University Plasma Physics Laboratory Report No. MATT-1038 (unpublished).

<sup>7</sup>T. Ohkawa, General Atomic Company Report No. GA-A13044 (to be published).

<sup>8</sup>J. C. Hosea, C. Bobeldijk, and D. L. Grove, in *Plasma Physics and Controlled Nuclear Fusion Research* (International Atomic Energy Agency, Vienna, Austria, 1971), Vol. II, p. 425.

<sup>9</sup>L. A. Artsimovich, *Nucl. Fusion* **12**, 215 (1972).

<sup>10</sup>V. S. Vlasenkov *et al.*, in *Proceedings of the Sixth European Conference on Controlled Fusion and Plasma Physics, Moscow, U. S. S. R., 1973* (U.S.S.R. Academy of Sciences, Moscow, U.S.S.R., 1973), Vol. I, p. 55.

<sup>11</sup>A divertor configuration has also been achieved in the JFT-2A experiment: T. Tazima *et al.*, in Proceedings of the Fifth International Conference on Plasma Physics and Controlled Nuclear Fusion Research, Tokyo, Japan, 1974 (International Atomic Energy Agency, Vienna, Austria, to be published), Paper No. CN-33/A1-2.

## Oxide-Charge-Induced Impurity Level in Silicon Inversion Layers

A. Hartstein and A. B. Fowler

*IBM Thomas J. Watson Research Center, Yorktown Heights, New York 10598*

(Received 14 April 1975)

We have observed a peak in the conductivity-versus-gate-voltage curves for  $n$ -channel silicon metal-oxide-semiconductor field-effect-transistor devices containing large oxide-charge densities,  $4.7 \times 10^{11} \text{ cm}^{-2} \leq N_{\text{ox}} \leq 1.1 \times 10^{12} \text{ cm}^{-2}$ . This peak is interpreted as an oxide-charge-induced impurity level within the lowest sub-band tail. It is found that the impurity level contains one electron state for each oxide charge situated at the Si-SiO<sub>2</sub> interface.

Many papers have been published recently on the channel conductivity of silicon metal-oxide-semiconductor field-effect-transistor (MOSFET) devices biased near threshold. The low-temperature conductivity has been shown to obey a  $\ln \sigma \propto T^{-1/3}$  relationship<sup>1,2</sup> for temperatures below 4.2°K. Recently, the present authors have shown<sup>3</sup> that this relationship can extend up to 77°K rather than changing to a  $\ln \sigma \propto T^{-1}$  law as previously thought. In the present paper we report the observation of peaked structure in the conductivity of  $n$ -channel silicon MOSFET devices in which

Na<sup>+</sup> ions have been placed at the Si-SiO<sub>2</sub> interface. Peaked structure in the field-effect mobility has previously been reported,<sup>4-6</sup> which seems to be unrelated to the present structure. We have also seen the peaked structure in the field-effect mobility and observed it to decrease in intensity at higher oxide-charge densities ( $N_{\text{ox}} > 4 \times 10^{11} \text{ cm}^{-2}$ ) where the new conductivity peak appeared.

The MOSFET devices used were prepared by standard techniques except that NaCl was evaporated into the gate oxide prior to the gate metal-

lization. The devices were fabricated on 2.0- $\Omega$ -cm *p*-type substrates, with an oxide thickness of 1000 Å. A known number of Na<sup>+</sup> ions were then drifted to the Si-SiO<sub>2</sub> interface and this distribution was frozen in. This allowed us to determine and control oxide-charge effects on a single device thus isolating effects due to surface roughness, etc., which may vary from device to device. The conductivity was measured by use of an ac technique which has been described elsewhere.<sup>4</sup> Conductivity was measured as a function of gate voltage, temperature, and oxide-charge density. The oxide-charge density was determined from the shift of the liquid-nitrogen transconductance threshold voltage from the zero-oxide-charge threshold. The inversion-layer carrier density was calculated from the difference between the gate voltage and the observed liquid-nitrogen threshold. This method has been shown to be reasonably consistent with Hall effect and oscillatory-magnetoconductance measurements.<sup>4</sup>

The new conductivity peak has been observed for oxide-charge densities in the range  $4.7 \times 10^{11} \text{ cm}^{-2} \leq N_{\text{ox}} \leq 1.1 \times 10^{12} \text{ cm}^{-2}$ . At the lowest density the peak was observed for temperatures between 10 and 24°K. For the highest density the peak was observed for temperatures between 4.2 and 33°K. The lower limits of both oxide-charge density and temperature on the peak observation are due to the sensitivity of the experimental apparatus. Figure 1 shows the conductivity as a function of gate voltage for  $T = 11.5^\circ\text{K}$  and  $N_{\text{ox}} = 7.2 \times 10^{11} \text{ cm}^{-2}$ . The separate curves have been obtained with different substrate biases, whose effect will be discussed later. The conductivity

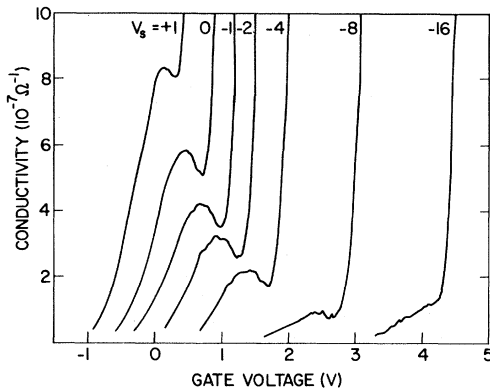


FIG. 1. Conductivity as a function of gate voltage for  $T = 11.5^\circ\text{K}$  and  $N_{\text{ox}} = 7.2 \times 10^{11} \text{ cm}^{-2}$ . Separate curves are for varying substrate bias.

peak is clearly evident. We next subtracted the estimated background conductivity from the observed conductivity in order to isolate the peak itself. The following results then apply to the peak itself.

The temperature dependence of the conductivity in the peak, as well as the background conductivity, obeys a  $\ln \sigma \propto T^{-1/3}$  law. This suggests a variable-range hopping mechanism.<sup>3</sup> The full width at half-maximum (FWHM) of the peak is found to involve two components: The first is temperature independent ( $\Gamma_0$ ) and the second increases approximately linearly with increasing temperature. The position of the peak is found to be independent of temperature. This position is in gate voltage, which can only be directly related to an energy scale if the density of states is independent of both temperature and screening effects.

The maximum conductivity of the peak was observed to increase rapidly with increasing oxide charge, following the approximate empirical relationship  $\sigma_{\text{max}} \propto N_{\text{ox}}^{6.5 \pm 0.5}$ . The temperature-independent part of the FWHM was found to obey the relationship  $\Gamma_0 \propto N_{\text{ox}}^{1/2}$ . This latter result suggests that the FWHM is proportional to the amount of local oxide-charge fluctuation. The difference in gate voltage between the positions of the mobility edge<sup>3</sup> ( $E_c$ ) and of the conductivity peak ( $E_i$ ) decreases with increasing oxide charge. Strictly speaking this means that the incremental number of inversion-layer electrons in the energy range  $E_c - E_i$  decreases. However, since the density of states can be assumed either to remain constant or to increase with oxide charge, the actual energy separation  $E_c - E_i$  decreases with increasing oxide charge.

In Fig. 1 the value of the conductivity peak is seen to decrease and finally saturate with a negative substrate bias. Note that the parallel shift of the conductivity curve in gate voltage reflects the shift in threshold voltage with substrate bias. It is instructive to obtain the total number of electrons in the inversion layer ( $N_{\text{INV}}$ ) corresponding to the conductivity peaks. This can be obtained from the equation

$$qN_{\text{INV}} = C_0(V_g - V_T), \quad (1)$$

where  $V_g$  is the gate voltage,  $V_T$  is the threshold voltage,  $q$  is the electronic charge, and  $C_0$  is the oxide capacitance. A plot of  $N_{\text{INV}}$  as a function of substrate bias is shown in Fig. 2.  $N_{\text{INV}}$  is also seen to decrease and eventually to saturate with negative substrate bias.

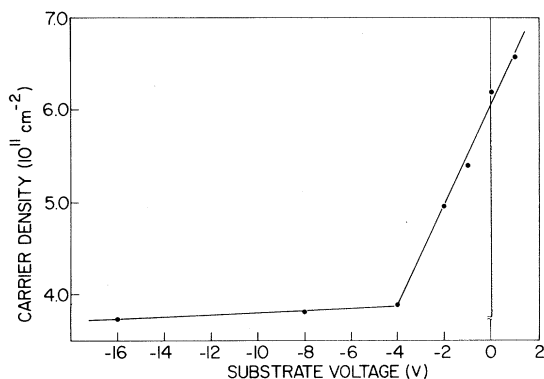


FIG. 2. Inversion-layer carrier density at the gate voltage corresponding to the conductivity peaks as a function of substrate bias.

All of these results may be interpreted in terms of an oxide-charge-induced impurity level which occurs within the band tail. This type of bound state has been discussed theoretically by Stern and Howard.<sup>7</sup> Our results are consistent with their lowest-lying bound state associated with the lowest sub-band.

Several of the results deserve further comment. The change in the separation  $E_c - E_i$  with oxide charge is particularly interesting. For an impurity level we can assume that, neglecting changes in the screening, the effect of increasing  $N_{ox}$  is to increase the number of states in the level, but to leave  $E_i$  essentially constant. Therefore, we can interpret the decrease of  $E_c - E_i$  with increasing oxide charge as a shifting of the mobility edge further into the band tail.

The conductivity within the oxide-charge-induced impurity band probably proceeds via a variable-range hopping mechanism since the density of states is still too low for extended-state band conduction and the  $T^{-1/3}$  law is observed experimentally. As the mobility edge moves closer to the impurity level the slope of the  $\ln\sigma$ -versus- $T^{-1/3}$  curves becomes smaller, indicating that the hopping is becoming easier. If the oxide-charge density can be increased enough without other effects such as sodium-ion agglomeration becoming important, the mobility edge should be seen to pass through the oxide-charge-induced impurity level.

The substrate-bias effects shown in Figs. 1 and 2 can be explained by considering the effect of substrate bias on the electrons. Negative sub-

strate bias has the effect of increasing the band bending at the surface and forcing the electrons closer to the surface. This causes the electrons to feel the ion electrostatic potential more strongly and causes an increase in the binding energy. The inversion-layer charge densities shown in Fig. 2 consist of a part due to the oxide-charge-induced impurity level and a part due to the band tail. The decrease in  $N_{INV}$  with negative substrate bias can then be interpreted in terms of the increase in binding energy of the impurity level relative to the band tail. Saturation of both  $N_{INV}$  and the conductivity occurs when the oxide-charge-induced impurity level is split off from the band tail.  $N_{INV}$  is then a measure of  $\frac{1}{2}$  the number of states in the impurity level (since  $N_{INV}$  is measured between the bottom of the level and the midpoint). In this way, the total number of states in the impurity level is determined to be  $7.8 \times 10^{11} \text{ cm}^{-2}$  which is nearly equal to the oxide-charge density ( $N_{ox} = 7.2 \times 10^{11} \text{ cm}^{-2}$ ).

We have shown that an oxide-charge-induced impurity level exists in  $n$ -channel silicon inversion layers. This level is distinct from the band tail and the associated wave functions are probably very different from those of the band-tail states. Both the number of states and their FWHM dependence suggest the  $\text{Na}^+$ -ion origin of the states. It would be instructive to look for the absence of such states in  $p$ -channel devices where a repulsive  $\text{Na}^+$ -ion potential will not produce the same type of bound state.

The authors wish to thank T. W. Hickmott and E. J. Petrillo for help in preparing the samples and H. Ripke for able technical assistance. They are further indebted to F. Stern for many valuable discussions.

<sup>1</sup>M. Pepper, S. Pollit, C. J. Adkins, and R. E. Oakley, *Phys. Lett.* **47A**, 71 (1974).

<sup>2</sup>D. C. Tsui and S. J. Allen, *Phys. Rev. Lett.* **32**, 1200 (1974).

<sup>3</sup>A. Hartstein and A. B. Fowler, *Bull. Amer. Phys. Soc.* **20**, 426 (1975), and to be published.

<sup>4</sup>F. F. Fang and A. B. Fowler, *Phys. Rev.* **169**, 619 (1968).

<sup>5</sup>N. Kotera, Y. Katayama, I. Yoshida, and K. F. Komatsubara, *J. Vac. Sci. Technol.* **9**, 754 (1972).

<sup>6</sup>R. J. Tidey and R. A. Stradling, *J. Phys. C: Proc. Phys. Soc., London* **7**, L356 (1974).

<sup>7</sup>F. Stern and W. E. Howard, *Phys. Rev.* **163**, 816 (1967).